applied sciences

MDPI

Article

Assessing Voltage Stability in Distribution Networks: A Methodology Considering Correlation among Stochastic Variables

Yuan Gao, Sheng Li * and Xiangyu Yan

School of Electric Power Engineering, Nanjing Institute of Technology, Nanjing 211167, China; gaoyuan6058@163.com (Y.G.); yanxiangyu0213@163.com (X.Y.)
* Correspondence: lisheng_njit@126.com

Abstract: Distributed photovoltaic (PV) output exhibits strong stochasticity and weak adjustability. After being integrated with the network, its interaction with stochastic loads increases the difficulty of assessing the distribution network's static voltage stability (SVS). In response to this issue, this article presents a probabilistic assessment method for SVS in a distribution network with distributed PV that considers the bilateral uncertainties and correlations on the source and load sides. The probabilistic models for the uncertain variables are established, with the correlation between stochastic variables described using the Copula function. The three-point estimate method (3PEM) based on the Nataf transformation is used to generate correlated samples. Continuous power flow (CPF) calculations are then performed on these samples to obtain the system's critical voltage stability state. The distribution curves of critical voltage and load margin index (LMI) are fitted using Cornish-Fisher series. Finally, the utility function is introduced to establish the degree of risk of voltage instability under different scenarios, and the SVS assessment of the distribution network is completed. The IEEE 33-node distribution system is utilized to test the method presented, and the results across various scenarios highlight the method's effectiveness.

Keywords: stochastic variable; correlation; voltage stability; probabilistic assessment

Citation: Gao, Y.; Li, S.; Yan, X. Assessing Voltage Stability in Distribution Networks: A Methodology Considering Correlation among Stochastic Variables. *Appl. Sci.* **2024**, *14*, 6455. https://doi.org/10.3390/app14156455

Academic Editors: Maria Vicidomini, Bogdan-Gabriel Burduhos, Gabriele Maria Lozito and Ahmed Elkafas

Received: 18 May 2024
Revised: 17 July 2024
Accepted: 22 July 2024
Published: 24 July 2024

1. Introduction

With the large-scale integration of distributed generators, line losses in the power grid have significantly decreased, and voltage configuration has been optimized [1]. However, the modern power system [2] must not only incorporate a high proportion of renewable energy, but also achieve high resilience, intrinsic safety, and reliability. Nevertheless, because renewable energy is unstable and load demand fluctuates stochastically [3], the power system faces severe challenges in maintaining secure and reliable performance [4]. The distribution network, positioned at the terminal of the power grid, is essential for conveying electricity from the transmission network to users of various voltage levels, making it the most critical link in guaranteeing the secure functioning of the power grid [5]. Therefore, to address the blind spot issues caused by the integration of distributed generators in traditional distribution network state assessment methods, it is critically important to study the stability of distribution networks with distributed generators [6].

SVS is essential for ensuring the overall stability of the distribution network [7]. The LMI is commonly used as an assessment indicator for voltage stability due to its clear physical meaning and ability to account for the nonlinearity of the system. Methods for calculating the load margin include the CPF method, internal point method, etc. [8]. However, traditional SVS studies are based on deterministic models, which do not consider the uncertainties of new energy sources and loads, making it impossible to analyze system stability accurately and effectively [9]. Therefore, it is necessary to research probabilistic

methods for assessing the SVS of a distribution network with uncertain new energy outputs and load fluctuations.

Currently, widely used probabilistic assessment methods include the Monte Carlo simulation (MCS) method, analytical method, and approximate method [10]. MCS primarily involves extensive stochastic sampling and repeated deterministic calculations for probabilistic analysis, providing clear physical significance, strong robustness, and high accuracy [11]. In [12], MSC was combined with dimensionally adaptive sparse grid interpolation to enhance computing efficiency. The MCS method is improved based on the ideas of dispersed sampling, which can significantly shorten calculation time by decreasing the sample size [13]. Although the above methods have improved computational efficiency while ensuring accuracy, the long processing time remains the biggest issue with the MCS method, and it generally serves as a control group to validate other methods. Widely used in analytical approaches are the semi-invariant method and the convolution method, the core of which is to linearize the relationships between stochastic variables for getting probabilistic characteristics of the variable values, resulting in faster solution speed [14]. Wang, Y [15] established a probabilistic power flow calculation method, taking into account load, and unit frequency characteristics based on the semi-invariant method. Reference [16] proposed an improved interval semi-invariant method to analyze the SVS margin for hybrid power grids with a large amount of new energy. Reference [17] used the maximum entropy principle and the semi-invariant method to research the comprehensive energy system of electric-gas interconnection with high efficiency, but it overlooked the influence of correlation factors among energy systems. Although the semi-invariant method has high computational efficiency, it involves complex mathematical calculations, and the convolution method is also difficult to implement, leading to suboptimal practical application results. The approximate method is to approximately analyze their numerical feature based on the distribution of the variables, with the point estimate method being a typical method [18]. Reference [19] utilized the point estimate method to obtain samples of stochastic variables and combined it with maximum entropy to determine their probability distribution, analyzing the impact of stochastic variables on system harmonics during the calculation of harmonic power flow. In [20], a surrogate-assisted point estimate approach was proposed to analyze the influence of mixed uncertainties on electric systems probabilistically. The point estimate method is extensively employed in the uncertainty evaluation of electric systems due to its short solving time, high accuracy, and the fact that it does not require knowledge of the specific functional relationships between variables.

In the operation of distribution networks, it is crucial to consider influences such as seasonal changes and weather conditions [21]. The solar radiation intensity at different locations in the same region and the load demands are not independent of each other but have certain correlations. These correlation factors significantly impact the operation of the distribution network [22]. Therefore, in conducting SVS analysis, it is imperative to not only account for the stochasticity of distributed generators but also for their correlations. Methods for addressing the correlation of stochastic variables include the Rosenblatt transformation [23], Orthogonal transformation [24], and the Nataf transformation [25]. Although the Rosenblatt transformation is applicable to any probability distribution, it requires detailed joint distribution data, which is challenging to acquire from practical engineering scenarios. Orthogonal transformation calculations are simple but only suitable for stochastic variables that obey normal distributions. The Nataf transformation has high computational accuracy, requiring only the marginal distributions and correlation coefficients of the stochastic variables, hence it has found widespread applications. Reference [26] combined the Nataf transformation with kernel density estimation to take the generator output power as input, and solve the probabilistic load flow using the point estimation method. However, the Pearson coefficient was used in the correlation treatment in the above literature, which cannot accurately describe the linear relationship between variables. The Copula function can accurately describe both linear and nonlinear relationships between variables. There is already research that combines MCS for probabilistic stability

analysis [27], but it is time-inefficient. Therefore, researching a probabilistic stability assessment method with high efficiency and an accurate description of the correlation between stochastic variables is essential.

Based on the above analysis, for the purpose of accurately characterizing the implications of uncertainty and correlation factors on SVS in distribution systems with distributed generators, a probability assessment method for SVS of distribution networks is proposed, which considers the uncertainties and correlations of the stochastic variables. The method presented in this article has the following main contributions:

- Unlike the traditional probabilistic voltage stability method, which disregards correlations, the method presented uses the Copula function to obtain the correlation coefficients of stochastic variables. The Frank Copula function can describe both the non-negative and negative correlations of variables;
- The 3PEM requires input variables to be mutually independent, thus it cannot handle correlated stochastic variables that follow arbitrary distributions in actual distribution networks. The proposed method uses the Nataf transformation to convert the correlated variable space into an independent standard normal space, which meets the applicability conditions of the 3PEM;
- Traditional power flow calculation can only calculate the node voltage and branch power. The load margin and critical voltage are important indexes to analyze voltage stability. The method proposed derives the probabilistic distribution information of these two indexes based on CPF calculation, which is more conducive to a thorough SVS analysis of the system;
- When PV is integrated into the system, stochastic variables in the system are not all normally distributed. The Cornish-Fisher series can be used to more accurately fit the distribution curves of non-normal distribution stochastic variables;
- The utility theory can nonlinearly represent the degree of risk of the system. The proposed method combines the utility function theory to define the extent of the LMI violations, quantify the voltage instability risk, and more intuitively show the current system's SVS.

2. Modeling of Stochastic Variables Considering Correlation

2.1. Probability Model for Stochastic Variables

2.1.1. Probabilistic Model of PV Generation

PV generation output is closely related to the solar irradiance in the area, and the solar irradiance is significantly affected by various factors including time, location, and cloud situations [28]. Therefore, its natural variability and time-varying lead to the instability of PV output. Research has shown that, over certain time scales, the stochastic variation characteristics of solar irradiance can be represented as Beta distribution, the probability density function (PDF) of which is [16]:

$$f(r) = \frac{\Gamma(\alpha+\beta)}{\Gamma(\alpha)\Gamma(\beta)}\left(\frac{r}{r_{\max}}\right)^{\alpha-1}\left(1-\frac{r}{r_{\max}}\right)^{\beta-1} \tag{1}$$

where $\Gamma()$ is the gamma function, r denotes the current solar irradiance at the location of the PV system, and $r_{\max}$ is the maximum irradiance during the period. α and β are shape parameters of the Beta distribution, and control the distribution curve together with the Gamma function, which can be calculated according to Equations (2) and (3):

$$\alpha = \mu\left[\frac{\mu(1-\mu)}{\sigma^2}-1\right] \tag{2}$$

$$\beta = (1-\mu)\left[\frac{\mu(1-\mu)}{\sigma^2}-1\right] \tag{3}$$

where μ represents the average solar irradiance received by the PV power field, and σ denotes the standard deviation.

It is considered that the PV active power output is approximately linear and operates in a constant power factor mode:

$$P_{\mathrm{PV}} = A \cdot r \cdot \eta \tag{4}$$

$$Q_{\mathrm{PV}} = \tan\phi_{\mathrm{PV}} \cdot A \cdot r \cdot \eta \tag{5}$$

where P_{PV} and Q_{PV} are the actual output power of PV power generation, A denotes the area of PV array, r represents actual light intensity, η signifies the conversion efficiency of PV power generation, while cosϕ represents the power factor during PV operation [29].

2.1.2. Probabilistic Model of Load

Research has indicated that fluctuations in the base load of power systems can be effectively described using a normal distribution. To better understand and predict changes of power system loads, a probability model of power based on normal distribution can be established [30]:

$$f(P) = \frac{1}{\sqrt{2\pi}\sigma_P} \cdot \exp\left[-\frac{(P-\mu_P)^2}{2\sigma_P^2}\right] \tag{6}$$

$$f(Q) = \frac{1}{\sqrt{2\pi}\sigma_Q} \cdot \exp\left[-\frac{(Q-\mu_Q)^2}{2\sigma_Q^2}\right] \tag{7}$$

Here, $f(P)$ and $f(Q)$ are probability density functions of active power and reactive power of stochastic load, respectively; μ_P, σ_P^2 and μ_Q, σ_Q^2 are the expected and variance of the power, representing the average level and fluctuation range of the power load, respectively.

2.2. Stochastic Variable Correlation Modeling

In the distribution network with integrated, distributed PV, the stochasticity of the variables mentioned is affected by multiple factors, including geographical location, climate conditions, and seasonal changes. These factors not only independently affect each variable but also lead to certain correlations among them. In the same distribution network, the locations of distributed PV are close to load points, and the external conditions are similar, so there is also a correlation within the variables. PV generators located in similar geographical areas are affected by similar climate conditions, showing certain correlations in their power output. Similarly, loads in neighboring areas may also show correlations due to similar climate conditions. To accurately simulate the correlations between these uncertain variables, including their linear and nonlinear dependencies, Copula functions are introduced for modeling correlation coefficients [27], thus flexibly describing and modeling various complex dependency relationships.

Copula theory is based on Sklar's theorem, which provides an accurate definition of Copula functions by Nelsen. Assuming there are n stochastic variables, X_1, X_2, $\cdots$, X_n, with their respective marginal distribution functions $F_1(x_1)$, $F_2(x_2)$, $\cdots$, $F_n(x_n)$, and their joint distribution function $H(X_1, X_2, \cdots, X_n)$, the Copula function, which serves as a connector between marginal and joint distributions, is defined as follows [31]:

$$H(X_1, X_2 \cdots X_n) = C(F_1(x_1), F_2(x_2), \cdots, F_n(x_n)) \tag{8}$$

where $C()$ is the Copula function. If there are stochastic variables with continuous marginal distribution functions, then a unique Copula function exists:

$$C(u_1, u_2, \cdots, u_n) = F\left(F_1^{-1}(u_1), F_2^{-1}(u_2), \cdots, F_n^{-1}(u_n)\right) \tag{9}$$

Copula theory provides a method that allows for accurately describing dependencies between variables, even when they have different marginal distributions. This approach offers greater precision compared to other methods.

Common Copula functions take many forms, as shown in Figure 1. The Archimedean Copula function is simple in form and can be uniquely determined by a convex function φ.

So, the problem can be simplified as follows: when used in high-dimensional situations, the rate and speed of convergence are higher [32]. Among them, the Gumbel and Clayton Copula functions cannot describe positive correlations, whereas the Frank Copula function can describe both positive and negative correlations [33]. Therefore, the Frank Copula function in Figure 1 is chosen to describe the correlation of stochastic variables in distribution networks with distributed generators [34]. Its cumulative distribution function (CDF) and PDF are, respectively, shown in Equations (10) and (11):

$$C_F(u,v,\theta) = -\frac{1}{\theta}\ln\left[1+\frac{\left(e^{-\theta u}-1\right)\left(e^{-\theta v}-1\right)}{\left(e^{-\theta}-1\right)}\right] \tag{10}$$

$$c_F(u,v,\theta) = \frac{-\theta\left(e^{-\theta}-1\right)e^{-\theta(u+v)}}{\left[\left(e^{-\theta}-1\right)+\left(e^{-\theta u}-1\right)\left(e^{-\theta_v}-1\right)\right]^2} \tag{11}$$

where θ is the correlation parameter of stochastic variables u and v.

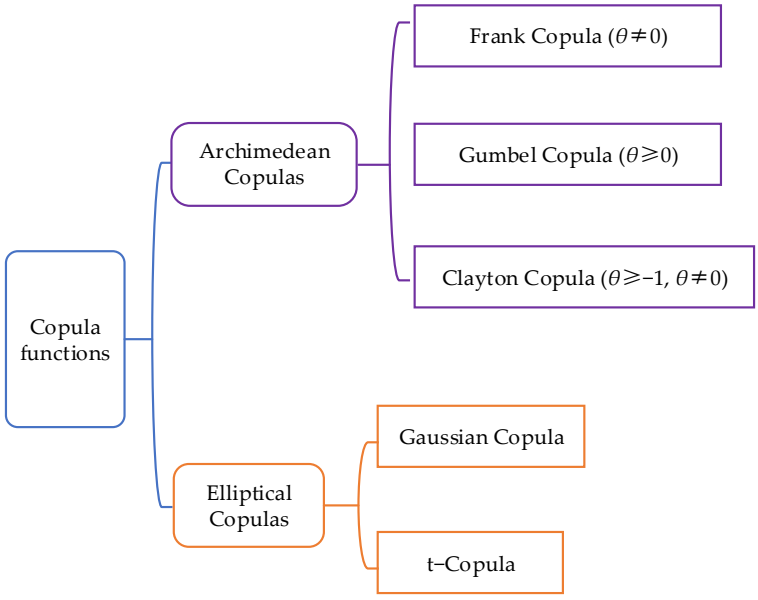

Figure 1. Types of Copula Functions.

The Kendall rank correlation coefficient τ can be derived instantly from these parameters of Copula function, making it especially suitable for application in Copula correlation models. The calculation equation is as follows:

$$\tau = 4\int_0^1\int_0^1 C(u,v)\mathrm{d}C(u,v) - 1 \tag{12}$$

To establish the correlation model for distribution network variables based on the Copula function, follow these specific steps:

Step 1: Obtain original data samples of distributed PV generators and loads;

Step 2: Choose the Frank Copula function to describe the correlations between the stochastic variables, based on the uncertainty of positive and negative correlations between PV and load data;

Step 3: Use the maximum likelihood estimation method derived from the initial sample's probability distribution, and apply Equations (10) and (11) to calculate the parameter θ of the Frank Copula function;

Step 4: Calculate the Kendall rank correlation coefficient τ using Equation (12), which serves as an index to measure the correlation between variables.

3. Probabilistic Assessment of Voltage Stability in Distribution Network Considering the Correlation of Stochastic Variables

To accurately characterize the influence of stochastic factors on SVS in the distribution network, the critical state of distribution network is first obtained through the CPF method [35], and then the probability distribution of LMI [7] is analyzed. The basic idea is: First, handle the correlated samples of input variables. Second, compute the sample values and weights using the 3PEM, conducting CPF calculations and obtaining the probabilistic distribution of the LMI using the corresponding series expansion method. Finally, establish the degree of risk of exceeding the index, and thus assess the SVS of the distribution network considering the correlation of stochastic variables.

3.1. Generating Correlated Samples Based on Nataf Transformation

When stochastic variables are correlated, 3PEM cannot directly sample. To generate samples with correlations, Nataf transformation is used to process the correlation of variables, which involves three steps. Namely, conversion between non-normally distributed input variables and correlated standard normally distributed input variables, transformation of the correlation coefficient matrix, and conversion between correlated standard normally distributed input variables and independent standard normally distributed input variables.

Assuming there is an n-dimensional stochastic variable $X = [x_1, x_2, \cdots, x_n]$ that follows arbitrary distributions, and the CDF of each stochastic variable x_i is $F_i(x_i)$, then, according to the principle of equal probability, the stochastic variable $Y = [y_1, y_2, \cdots, y_n]$ subject to the standard normal distribution can be obtained from Equation (13).

$$y_i = \Phi^{-1}(F_i(x_i)) \tag{13}$$

In Equation (13), Φ^{-1} represents the inverse of the CDF.

The correlation coefficient matrix for X is p and for Y is p_0. According to the Nataf transformation, the corresponding elements p_{ij} and p_{0ij} (where $i \neq j$) of p and p_0 are not equal [25], and this relationship is shown in Equation (14):

$$\begin{aligned} p_{ij} &= \int_{-\infty}^{+\infty}\int_{-\infty}^{+\infty}\frac{x_i-\mu_i}{\sigma_i}\cdot\frac{x_j-\mu_j}{\sigma_j}f_{ij}(x_i,x_j)dx_i dx_j \\ &= \int_{-\infty}^{+\infty}\int_{-\infty}^{+\infty}\frac{F_i^{-1}(\Phi(y_i))-\mu_i}{\sigma_i}\cdot\frac{F_j^{-1}(\Phi(y_j))-\mu_j}{\sigma_j}.\phi(y_i,y_j,p_{0ij})dy_i dy_j \end{aligned} \tag{14}$$

where μ_i, μ_j, σ_i, and σ_j, respectively, denote the means and standard deviations of the stochastic variables x_i and x_j; ϕ (y_i, y_j, p_{0ij}) is the joint PDF of a two-dimensional standard normal distribution with p_{0ij}.

Because the correlation coefficient matrix p_0 is a symmetric positive definite matrix, the lower triangular matrix L is acquired through Cholesky decomposition.

$$p_0 = LL^{\mathrm{T}} \tag{15}$$

After obtaining the correlated standard normal stochastic variables Y and matrix L, we can derive the independent standard normal stochastic variables $Z = [z_1, z_2, \cdots, z_n]$ from Equation (16):

$$Z = L^{-1}Y \tag{16}$$

The process described above, where correlated stochastic variables X that follow any distribution are transformed into independent standard normal variables Z, is known as the Nataf transformation. The samples of correlated stochastic variables that adhere to arbitrary distributions are constructed on the basis of the Nataf inverse transformation. The samples are obtained using Equation (17) [36]:

$$X = F^{-1}(\Phi(LZ)) \tag{17}$$

3.2. 3PEM Considering Variable Correlation

Considering the superiority of the point estimation method in dealing with uncertain factors, this paper adopts 3PEM for probabilistic voltage stability analysis. The basic idea of the 3PEM is: Given the probability distributions of the input variables on the condition that they are mutually independent, three sampling points are taken from each input stochastic variable to reflect probability and statistical characteristics of the variables. The output samples are calculated according to the functional relationship between the input and output variables. Subsequently, origin moments at each order of the output variables are determined, and probability distributions of the output variables are acquired through fitting [19].

Assuming G is the m-dimensional output variable and x_i (i = 1, 2, ⋯, n) are the input stochastic variable, then:

$$G = P(X) = P(x_1, x_2, \cdots, x_n) \tag{18}$$

In Equation (18), P is the correlation function of G and X, where $G = [g_1, g_2, \cdots, g_n]^{\mathrm{T}}$.

According to the principle of 3PEM, three sampling values of each stochastic variable x_i in independent standard normal space are obtained, $x_{i,k}$ (k = 1, 2, 3), and the sampling calculation equation is as follows [20]:

$$x_{i,k} = \mu_{xi} + \xi_{xi,k}\sigma_{xi} \quad k = 1, 2, 3 \tag{19}$$

where μ_{xi}, $\xi_{xi,k}$, and σ_{xi} represent the expected value, location coefficient, and standard deviation of stochastic variable x_i, respectively, where location coefficient $\xi_{xi,k}$ can be expressed as:

$$\begin{cases} \xi_{xi,k} = \frac{\lambda_{i,3}}{2} + (-1)^{3-k}\sqrt{\lambda_{i,4} - \frac{3}{4}\lambda_{i,3}^2} & k = 1, 2 \\ \xi_{xi,3} = 0 \end{cases} \tag{20}$$

where $\lambda_{i,3}$ represents the third-order moment of variable x_i, known as the skewness coefficient. $\lambda_{i,4}$ represents the fourth-order moment, known as the kurtosis coefficient, and is expressed as:

$$\begin{cases} \lambda_{i,3} = \frac{\mathrm{E}\left[\left(x_{i,k} - \mu_{xi}\right)^3\right]}{{\sigma_{xi}}^3} \\ \lambda_{i,4} = \frac{\mathrm{E}\left[\left(x_{i,k} - \mu_{xi}\right)^4\right]}{{\sigma_{xi}}^4} \end{cases} \tag{21}$$

The weight coefficient corresponding to each sampling point is:

$$\begin{aligned} w_{xi,k} &= \frac{(-1)^{3-k}}{\xi_{xi,k}\left(\xi_{xi,1} - \xi_{xi,2}\right)} \quad k = 1, 2 \\ w_{xi,3} &= \frac{1}{n} - \frac{1}{\lambda_{i,4} - \lambda_{i,3}^2} \end{aligned} \tag{22}$$

Through the above process, 3n sampling points can be obtained, so 3n deterministic evaluations need to be performed. However, when k = 3 and $x_{i,k} = \mu_{xi}$, only one calculation is needed, hence there are only (2n + 1) samples, and only (2n + 1) evaluations need to be performed. Using the Nataf inverse transformation, which is employed in Section 3.1, to transform the sample correlations before input, and integrating the above results [37], the l-order origin moment of the output variable g_j is $E(g_{lj})$:

$$E\left(g_j^l\right) \approx \sum_{i=1}^{n}\sum_{k=1}^{2} w_{xi,k}\left(g_j(i,k)\right)^l + w_{2n+1}g_{2n+1}^l \tag{23}$$

From Equations (24) and (25), the mean μ_{gi} and standard deviation σ_{gi} can be calculated as:

$$\mu_{gj} = E\left(g_j\right) \quad j = 1, 2, \cdots, n \tag{24}$$

$$\sigma_{gj} = \sqrt{E\left({g_j}^2\right) - {\mu_{gj}}^2} \quad j = 1, 2, \cdots, n \tag{25}$$

The steps for the 3PEM based on the Nataf inverse transformation are as follows:

Step 1: Determine the input stochastic variable $X = [x_1, x_2, \cdots, x_n]$ and the correlation coefficient matrix p_x, solve the correlation coefficient matrix p_y of standard normal stochastic variable Y, and obtain matrix L through Cholesky decomposition.

Step 2: Determine the location coefficients and weight coefficients for the sampling points in the independent standard space based on the principle of 3PEM. Construct $(2n + 1)$ matrices $Z = [Z_{1,1}, Z_{1,2}, \cdots, Z_{n,1}, Z_{n,2}, Z_{2n+1}]$ in the form of vectors $Z_{ik} = [0, 0, z_{i,k}, 0, 0]^{\mathrm{T}}$.

Step 3: Perform the Nataf inverse transformation to obtain the point estimation matrix $X = [x_{1,1}, x_{1,2}, \cdots, x_{n,1}, x_{n,2}, x_{2n+1}]$ in the original variable space corresponding to Z.

Step 4: Insert each column of X elements into Equation (18) to obtain the $(2n + 1)$ output result of G, and estimate its standard deviation and expectation.

3.3. Cornish-Fisher Series

With the aim of acquiring the distribution function characteristics of the LMI, semi-invariants calculated from the origin moments derived in Section 3.2 were utilized. Combining these with the Cornish-Fisher expansion series allows for the determination of the PDF and CDF of these outcome stochastic variables. However, semi-invariants, as numerical characteristics, are challenging to calculate directly. Finite order semi-invariants are obtained through corresponding to the origin moment α:

$$\begin{cases} \kappa_1 = \alpha_1 \\ \kappa_m = \alpha_m - \sum\limits_{j=1}^{m-1} C_{m-1}^{j} \alpha_j \kappa_{m-j}, \quad m = 2, 3, \cdots \end{cases} \tag{26}$$

where κ represents the semi-invariant of the stochastic variable, C_{m-1}^{j} are binomial coefficients, and α_i are the origin moments of the stochastic variable.

Once the semi-invariants of variable X are known, it is essential to ensure the accuracy of the fitted curve. The Cornish-Fisher expansion series is effective and precise in fitting probability distributions of non-normally distributed variables due to its good convergence properties. So, the probability distribution is derived through the Cornish-Fisher series expansion approximation, where $x(\theta)$ can be expressed as [38]:

$$\begin{aligned} x(\theta) = \zeta(\theta) + \tfrac{\zeta(\theta)^2 - 1}{6}\kappa_3 + \tfrac{\zeta(\theta)^3 - 3\zeta(\theta)}{24}\kappa_4 + \\ \tfrac{2\zeta(\theta)^3 - 5\zeta(\theta)}{36}\kappa_3^2 + \tfrac{\zeta(\theta)^4 - 6\zeta(\theta)^2}{120}\kappa_5 + \ldots \end{aligned} \tag{27}$$

Here, $\zeta(\theta) = \varphi^{-1}(\theta)$, φ denotes the CDF of the standard normal distribution. From $x(\theta) = F^{-1}(\theta)$, the CDF $F(x)$ of the stochastic variable X should be obtained, from which the PDF can be derived through differentiation.

3.4. Risk Preference Assessment Indicator

The risk index can quantitatively reflect the system's security state by synthesizing the probability of incident occurrence and the severity of its aftermath. This paper adopts a risk preference utility function based on utility theory, and constructs a severity function model in conjunction with the exceedance of the LMI. This allows the quantitative calculation of the risk of static voltage instability, thereby enabling the accurate assessment of voltage stability in the distribution network with distributed generators [39].

The severity function $S(I_{\mathrm{LM}})$ of the load margin index I_{LM} is defined as [39]:

$$S(I_{\mathrm{LM}}) = \frac{\mathrm{e}^{h(I_{\mathrm{LM}})} - 1}{\mathrm{e} - 1} \tag{28}$$

Here, I_{LM} is the LMI of the distribution network. The calculation formula of the index lower limit $h(I_{LM})$ is as follows:

$$h(I_{LM}) = \begin{cases} (I_c - I_{LM})/(1 - I_c), I_{LM} < I_c \\ 0, I_{LM} \geq I_c \end{cases} \quad (29)$$

where I_c is the alarm limit of I_{LM} index. The severity function curve under this definition is shown in Figure 2.

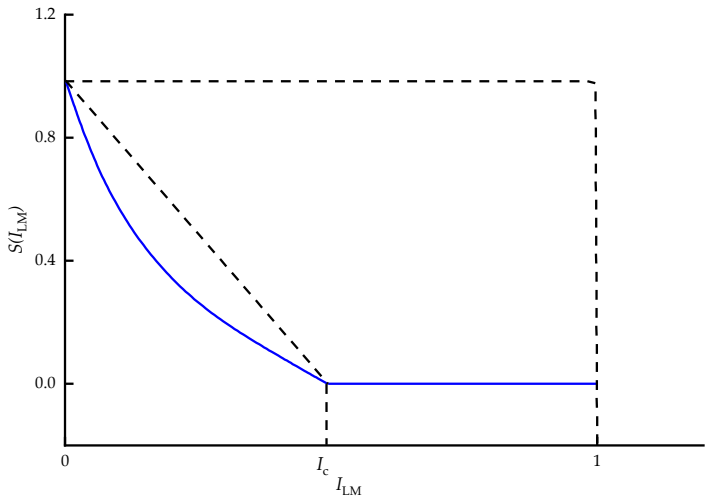

Figure 2. Curve of the severity function S(I_{LM}).

Combined with the probability density function $f(I_{LM})$ of I_{LM} index, the system static voltage instability risk can be defined as R, according to the I_{LM} index-exceedance risk [40]:

$$R = \int f(I_{LM}) S(I_{LM}) \mathrm{d}I_{LM} \quad (30)$$

Using R as an indicator, it is possible to effectively analyze the impact of the stochasticity of PV output and load power on the load margin, as well as the system-operational risks of the distribution network under different PV connection methods and capacities.

4. Assessment Process

The probabilistic assessment method of the SVS of a distribution network proposed by this paper utilizes the Copula function and Nataf transformation to address correlations between variables. The 3PEM was used to select samples for CPF calculations, transforming complex uncertainty issues into determinate issues. Finally, combined with the load margin index I_{LM}, the probabilistic voltage-stability assessment of the distribution network with distributed generators was completed. The computational process is illustrated in Figure 3, with detailed steps as outlined below:

Step 1: Establish typical probability models for PV generators and load, and the Copula correlation coefficient matrix p_{ij} between the stochastic variables.

Step 2: Sample the input variables in the independent standard normal distribution space. Calculate the position and weight coefficients of each input variable's estimated point according to 3PEM.

Step 3: Cause the matrix Z to be evaluated within the independent standard normal space, and use the Nataf inverse transformation to convert it back into the original correlated variable space, obtaining the assessment matrix X.

Step 4: Carry out CPF calculations with every column of the evaluation matrix X as input samples to determine the corresponding voltage stability critical values V_{cr} and load margin index I_{LM}. From Equations (23)–(25), their expected values, standard deviations,

and raw moments are obtained, and the distribution model of critical value V_{cr} and the PDF of I_{LM} index are obtained by the Cornish-Fisher series expansion.

Step 5: Apply a risk preference function as specified in Equation (28) to obtain the severity function, and combine it with the PDF from Step 1 to calculate the index-exceedance risk of the distribution network, thus completing the SVS assessment of the distribution network with distributed generators.

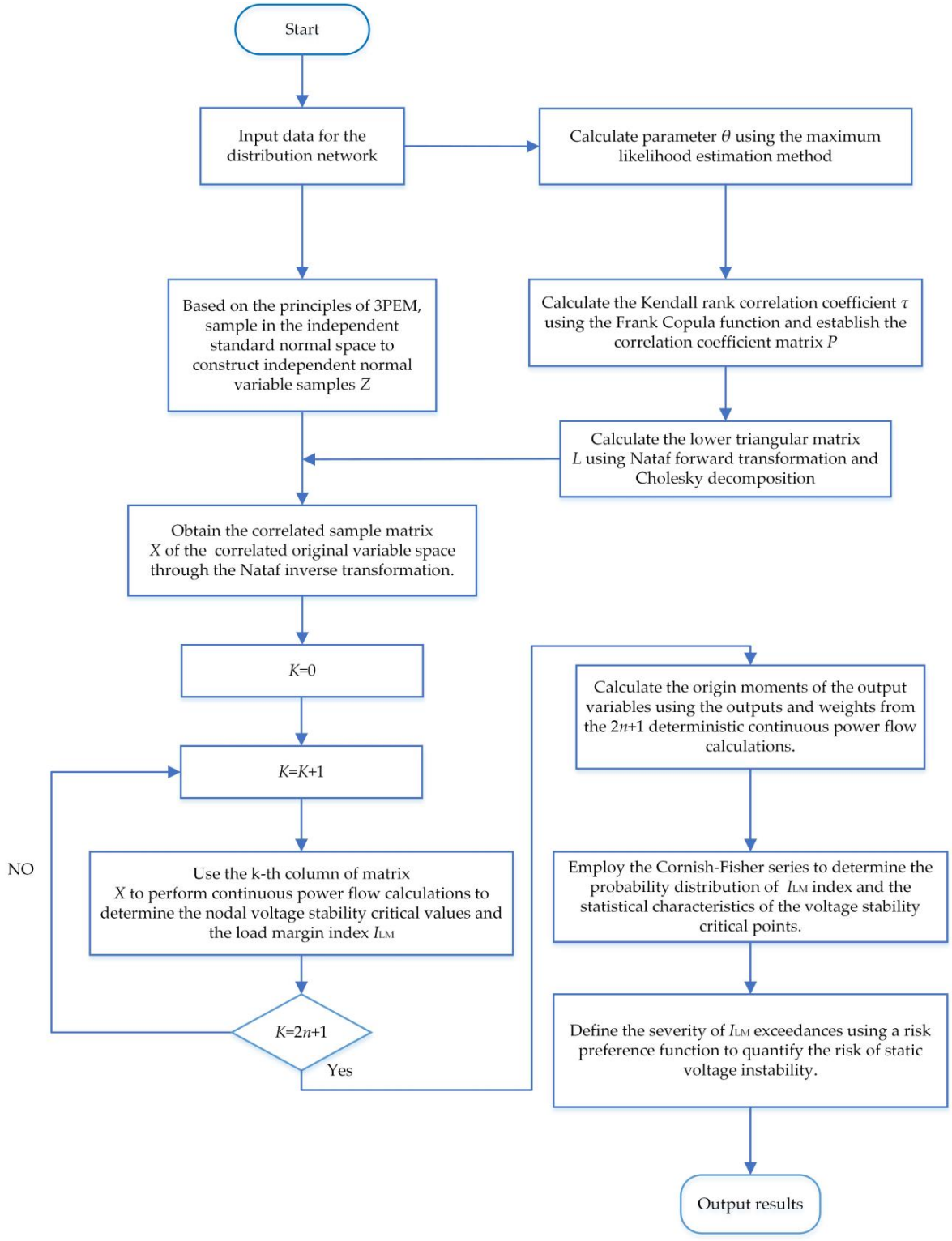

Figure 3. Process for SVS probability assessment.

5. Case Analysis

This paper conducts a case study of a distribution network with distributed PVs, using the IEEE 33-node distribution system as an example to validate the effectiveness of the proposed voltage stability assessment method [41]. Figure 4 illustrates the topology of the distribution network.

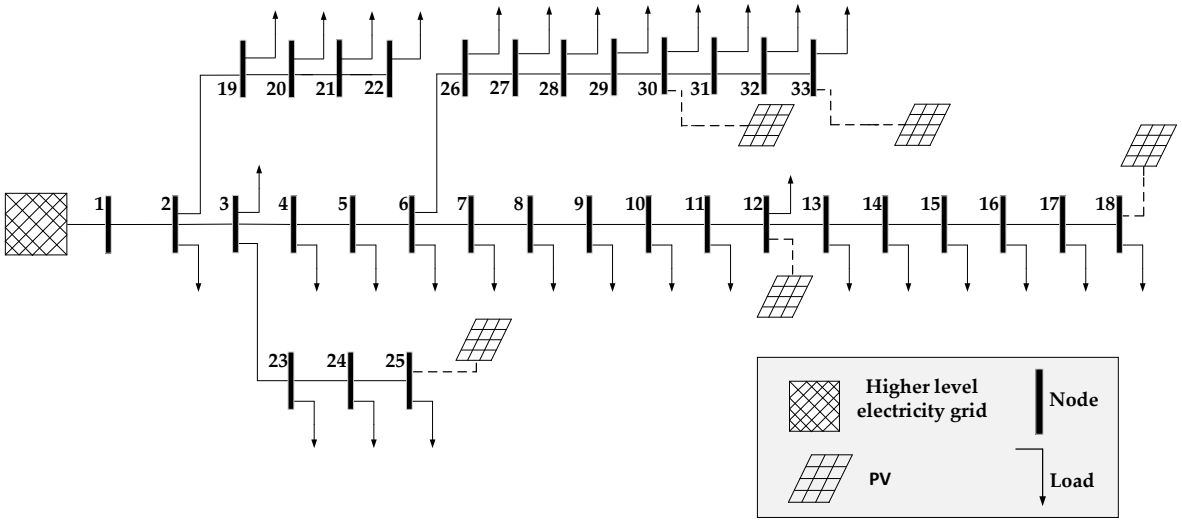

Figure 4. IEEE 33-node distribution system with distributed PVs.

The IEEE 33-node system has a total of 32 branches with a base power of 10MVA and a base voltage of 12.66 kV, where node 1 is set as the slack node. The loads follow normal distribution with the expected values by referring to the IEEE 33-node standard test system, and the standard deviation is set at 10% of the expected values. In Figure 4, PV represents distributed PV, and dashed lines indicate the options for connection, thereby facilitating discussions of future scenarios. PV output obeys Beta distribution, which is calculated as the PQ node. The shape parameters are α = 3.613, β = 5.938. The PV conversion efficiency is η = 13.44%.

The proposed model was established using MATLAB R2021b and the Matpower 7.1 toolkit. In the MATLAB coder, the power models for the load and PV were constructed through coding. The Matpower software package was then used to import the model data of the IEEE 33-node system, and the continuous power flow calculation and stochastic analysis were carried out to evaluate the voltage stability of the distribution network. The testing system was implemented on a computer (Manufactured by Lenovo Group and purchased in Xuzhou, China) with an Intel i7-7700HQ CPU (2.8 GHz) and 16 GB of RAM.

Without considering the stochastic factors, the CPF calculation was performed by gradually increasing the load at each node in proportion, while maintaining a constant power factor. The λ-V curve of each node in the system can be obtained by calculation, and the voltage-stability critical point of the node can be obtained. Taking the curve of Node 16 as an example, as shown in Figure 5.

In Figure 5, λ is called the load parameter, which is the ratio of the active power absorbed by the load at a certain moment to the base state active power. V_{cr} is the critical voltage of the node.

This paper takes the IEEE 33-node distribution system with PV as a case study, considering the uncertainties of both PV and load. The stability critical state of each node in the system was obtained through CPF calculation. The load margin index I_{LM} was obtained according to λ, and the probability distribution model was set up to complete the probabilistic assessment of voltage stability.

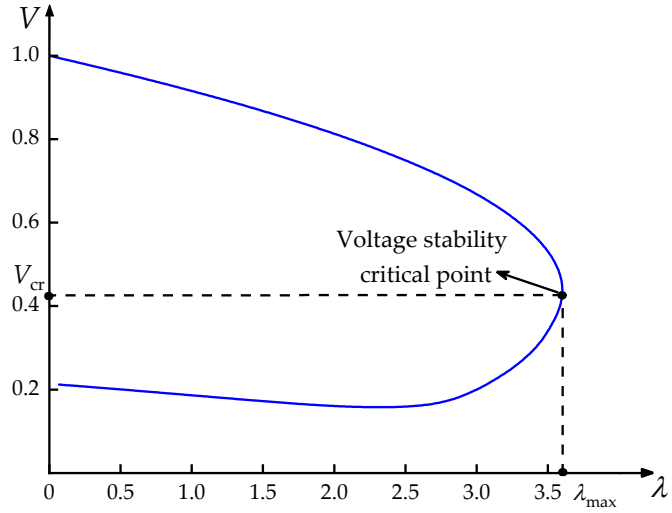

Figure 5. λ-V curve of Node 16.

5.1. Method Verification

To validate the calculation effect of the method presented in various scenarios of PV integration into the distribution network, the following three scenarios were defined:

- Scenario 1: PV generators are centrally connected to node 33, and a total connection capacity of 1.5 MW;
- Scenario 2: PV generators are dispersedly connected to nodes 33, 30, 25, 18, and 12, with each node having a rated output of 0.2 MW and a total network connection capacity of 1 MW;
- Scenario 3: PV generators are dispersedly connected to nodes 33, 30, 25, 18, and 12, with each node having a rated output of 0.3 MW, and a total network connection capacity of 1.5 MW.

A considerable amount of Monte Carlo simulations were carried out, and it was found that the results tended to be stable after 5000 sampling instances. With the aim of validating the precision and efficiency of the method, results from the MCS using 5000 samples were used as a comparison. The proposed method, the traditional 3PEM method, and the MCS method, were then used to perform probabilistic analyses of the distribution network system under the three scenarios described. To calculate the voltage stability critical points, it was assumed that the entire system load grew at a constant power factor. Figures 6–8 present the voltage stability critical values at various nodes, and the cumulative distribution functions the system LMI for the three scenarios using different methods.

In these figures, Case 1 employs the MCS method, taking into account variable correlations (5000 samples); Case 2 uses the method proposed by this paper, considering variable correlations; Case 3 uses the traditional 3PEM, without considering variable correlations.

The simulations demonstrate that the presented method can precisely calculate the voltage stability critical values at each node and the load margin of the entire network when the loads at all nodes uniformly increase according to a constant power factor.

From (a) in Figures 6–8, it is evident that, as distributed photovoltaics are integrated into the distribution network, the overall voltage at network nodes increases, and the increase is more pronounced the closer to the connection node they draw. This integration improves the SVS in the distribution network. However, centralized single-point connections can lead to voltage exceedances as capacity increases, posing a threat to the stable operation of the distribution network. Dispersed multi-point connections more effectively limit voltage fluctuations, maintaining the reliable and stable operation of the system. Comparing the three methods in each scenario, the curve for Case 2 essentially coincides with that of Case 1, while the curve for Case 3 shows a slight deviation. Moreover, as the

number of stochastic variables and the connection capacity increase, the deviation becomes more significant.

In (b) of Figures 6–8, by comparing the CDF for across the three scenarios as the dimension of stochastic variables and capacity increase, we see the fitting effectiveness of the traditional 3PEM deteriorates, and the error relative to the MCS method grows larger. In contrast, the curves fitted by the proposed method has a high fit with the benchmark method (MCS), and its probability distribution can be accurately obtained, which proves the effectiveness of the method.

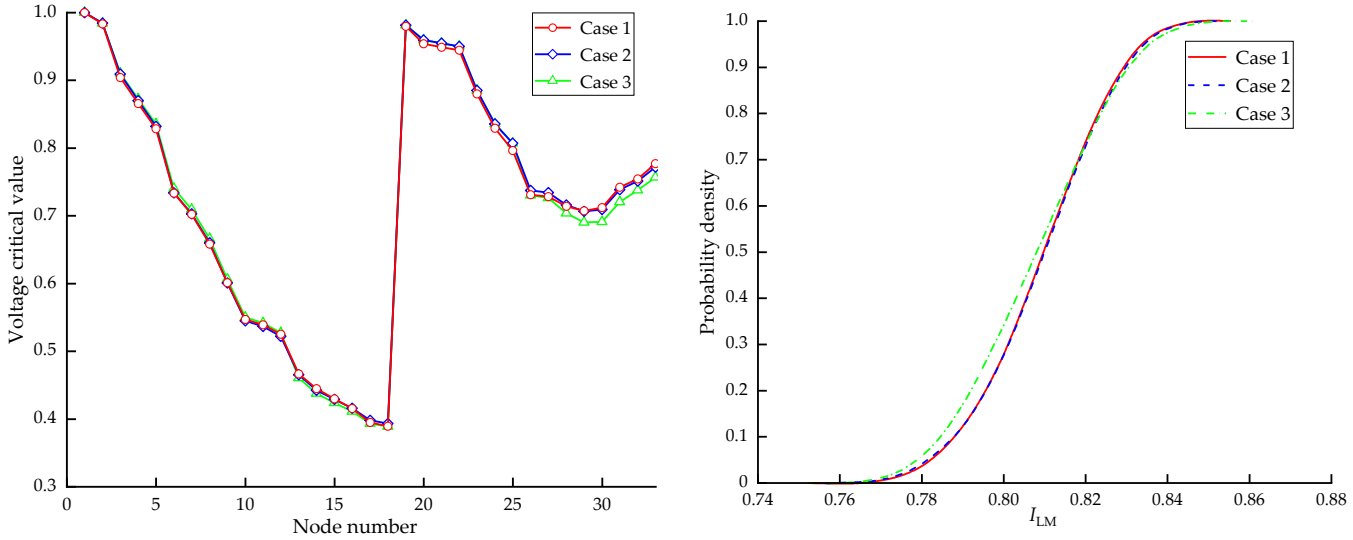

Figure 6. Node voltage stability critical value and CDF of I_{LM} index in Scenario 1: (**a**) voltage stability critical values at each node; (**b**) CDF of I_{LM} index.

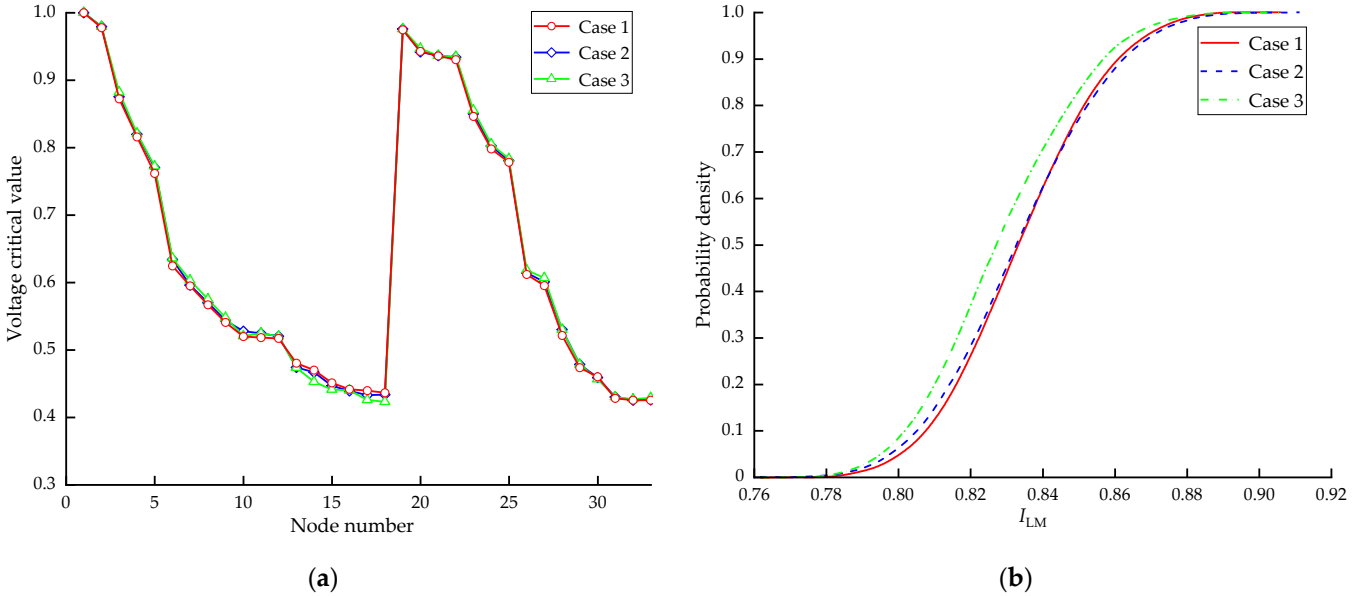

Figure 7. Node voltage stability critical value and CDF of I_{LM} index in Scenario 2: (**a**) voltage stability critical values at each node; (**b**) CDF of I_{LM} index.

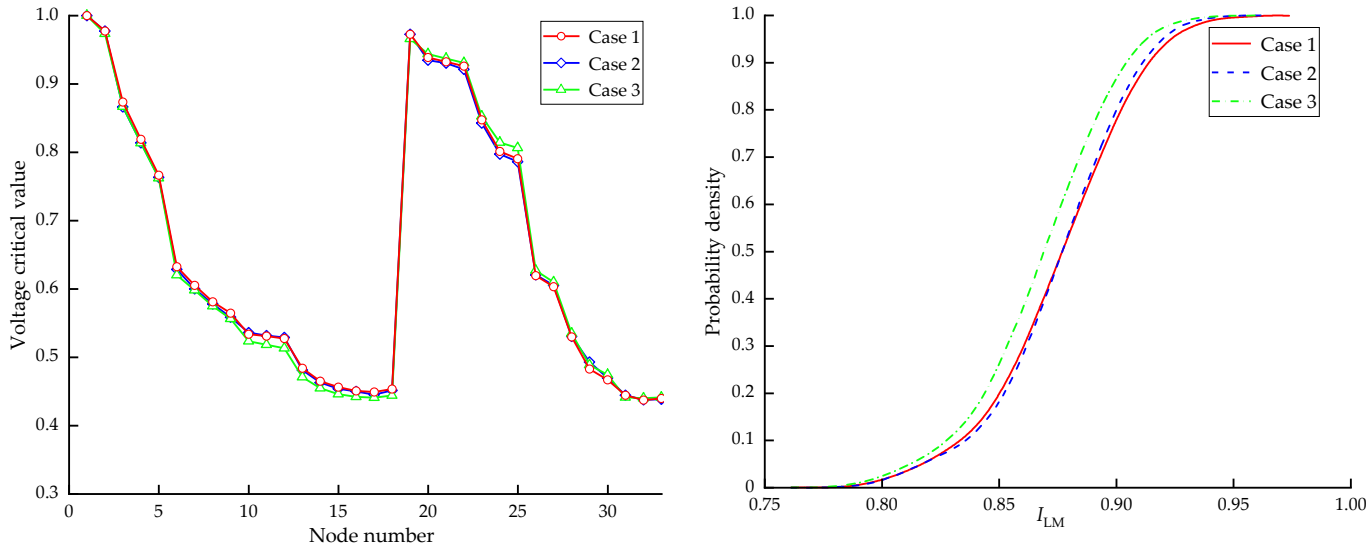

(**a**) (**b**)

Figure 8. Node voltage stability critical value and CDF of I_{LM} index in Scenario 3: (**a**) Voltage stability critical values at each node; (**b**) CDF of I_{LM} index.

To further verify the computational accuracy of the method presented, the relative error indicators ε_μ for the expected value, and ε_σ for the standard deviation of the I_{LM} index, as shown in Equations (31) and (32) [37], are used as accuracy-assessment indicators for the method proposed in this paper.

$$\varepsilon_\mu = \left| \frac{\mu_{MCS} - \mu_{PEM}}{\mu_{MCS}} \right| \times 100\% \tag{31}$$

$$\varepsilon_\sigma = \left| \frac{\sigma_{MCS} - \sigma_{PEM}}{\sigma_{MCS}} \right| \times 100\% \tag{32}$$

where μ_{MCS} and μ_{PEM} are the expected values of the I_{LM} index obtained by the MCS and 3PEM methods, respectively. σ_{MCS} and σ_{PEM} are the standard deviations of the I_{LM} index as calculated by the MCS and 3PEM methods, respectively.

From the statistical data in Table 1, it is observed that the relative error in the expected values of the algorithm proposed in this paper do not exceed 0.2%, and the relative error in the standard deviation is less than 1.18%. The calculation results are essentially consistent with those acquired by the MCS method, effectively reducing the fitting errors of the two methods, indicating that the proposed method achieves high accuracy in the statistical characteristics of output variables. Generally, the error in the estimated standard deviation of the output variable is greater than that of the estimated expected value, which accords with the characteristics of the point-estimation method.

Taking Scenario 3 as an example, Table 2 presents the simulation times for the three methods. The data indicate that, due to the consideration of correlations, the simulation time required by the presented method is slightly slower than that of the 3PEM, which does not consider correlations. However, compared to the MCS method, the method algorithm still significantly reduces the amount of time required. Therefore, considering both calculation time and precision, the method proposed by this paper is a highly precise and time-effective SVS probabilistic assessment method.

Table 1. Relative errors in the expected value and standard deviation of I_{LM} derived from two kinds of point-estimation methods.

Scenario	3PEM Considering Correlations		3PEM Without Considering Correlations	
	Relative Error of the Expected Value%	Relative Error of the Standard Deviation%	Relative Error of the Expected Value%	Relative Error of the Standard Deviation%
Scenario 1	0.09	0.76	0.32	3.12
Scenario 2	0.136	1.09	0.63	4.473
Scenario 3	0.153	1.18	0.78	4.96

Table 2. Comparison of simulation time among three methods.

Methods	MCS (5000)	3PEM Considering Correlations	3PEM Without Considering Correlations
Time (s)	7086.5	56.62	50.86

5.2. Probabilistic Voltage Stability Assessment under Different Scenarios

The method proposed by this paper was employed for carrying out probability assessment of LMI under different scenarios, and the PDF and change trend of the indexes were obtained, as shown in Figure 9. Since the input variables contained non-normal variables, the probability density curves of the stability margin exhibited non-normal characteristics. Additionally, as the capacity of photovoltaic integration increases, the probability curves of the margin index generally shift to the right, and their values increase. It is evident that, within a reasonable range of photovoltaic grid-connected capacities, the larger the capacity, the more significant its role in enhancing the system's operational stability. Furthermore, with relatively lower connection capacities, the dispersed integration of PV generators into the system displayed a broader load margin. The wider distribution indicates that, under various operating conditions, the network exhibited higher variability but typically maintained higher stability, and the power grid had a greater ability to adapt to load changes.

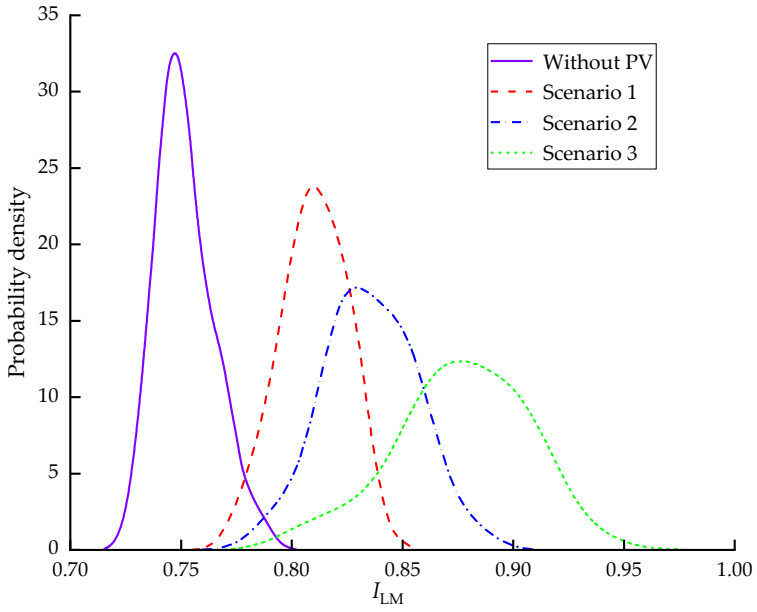

Figure 9. Probability density curves of I_{LM} under different scenarios.

In the scenarios with distributed generators integrated into the distribution network, the LMI also displayed a heavier tail distribution, which means that the grid had a higher probability of maintaining a high load-margin under extreme conditions. This was due to multi-point power generation, which could be supplemented by other nodes when some nodes were affected by load or failure, thereby enhancing the overall resilience of the grid and making it more stable in the face of a wide range of operating conditions and potentially high-load events. In contrast, scenarios with centralized access to the distribution network showed a lighter tail, which meant that, under extreme load conditions, the network had difficulty maintaining a high load-margin, increasing the risk of grid collapse in the face of high loads or failures. Particularly in Scenario 3, the higher overall capacity and distributed configuration significantly enhanced the load margin, enabling the grid to better withstand various load fluctuations, and thus enhancing overall stability.

In the aforementioned distribution network system scenarios, a warning value for the I_{LM} was set at 0.8. Therefore, the severity function of the LMI and the PDF of I_{LM} were used to calculate the static voltage instability risk, and the outcomes are presented in Table 3.

Table 3. Degree of risk of static voltage instability.

PV Integration Scenario	Degree of Risk of Static Voltage Instability		
	MCS (5000)	3PEM Considering Correlations	3PEM without Considering Correlations
Without PV Integration	0.2372	0.2370	0.2379
Scenario 1	0.0277	0.0275	0.0287
Scenario 2	0.0135	0.0138	0.0149
Scenario 3	0.0019	0.0017	0.0035

Analysis of the data shows that the instability risk calculated by the 3PEM considering correlations is essentially consistent with the MCS (5000) method. Although the traditional 3PEM can also identify the degree of instability in various scenarios, there are still discrepancies compared to the MCS method. Therefore, the better the fitting effect of I_{LM} probability distribution, the more accurate the results of the system stability assessment, which also verifies the precision of the method presented.

Comparing values of each scenario, Scenario 3 shows the lowest risk due to its high and widespread I_{LM} values. This indicates that adopting distributed PV integration and ensuring higher connection capacities can improve the load margin and thus effectively reduce the risk of voltage instability. In contrast, centralized access systems, while simplifying management and maintenance, may face a higher risk of instability due to low load-margins.

6. Conclusions

This paper analyzed the uncertainty and correlation of distributed generators and loads within the distribution network. Addressing the shortcomings of traditional probability assessment methods to deal with the correlation between variables, the Copula function and Nataf transformation were introduced into 3PEM, combined with the load margin index I_{LM} and a risk-preference utility function, to propose a probabilistic assessment method for SVS that accurately handled the correlations among input variables. The IEEE 33-node power distribution system was connected to distributed PV for testing, and the conclusions are as follows:

(1) Across different distribution functions, the proposed method accurately handled the correlations among input variables, demonstrating strong applicability, high computational efficiency, and precision;

(2) Combined with the risk-preference utility function, the degree of risk of voltage instability of the system was established, which can be a more comprehensive and quantitative assessment of the operational risks of a distribution network with distributed generators in different scenarios;
(3) Distributed access not only enhances the stability of the electrical grid but also improves the performance of the grid under extreme conditions by spreading risk and enhancing system redundancy. Therefore, distributed access strategies should be prioritized in the design and planning of modern distribution networks.

The case of the IEEE 33-node system provides validation that the method presented significantly improves computational efficiency compared to the MCS method, while maintaining high accuracy. This method is suitable for analysis and calculation tasks such as safe operation, planning, and scheduling of distribution networks under strong uncertainties on both the source and load sides. It provides more comprehensive and accurate auxiliary decision-making information for planning and scheduling personnel, thus having practical engineering application value. However, it should be noted that the proposed method does not involve the ring network structure for voltage stability analysis of the distribution network, which presents certain limitations. As part of future research, we will extend the study to distribution network systems with ring structures. By researching different network topologies and optimizing control strategies, we further enhanced the comprehensiveness and practicality of the study, providing a stronger guarantee for the safe operation and optimized dispatch of the power system.

Author Contributions: Conceptualization, S.L. and Y.G.; methodology, Y.G. and S.L.; software, Y.G. and X.Y.; validation, S.L. and Y.G.; formal analysis, S.L., Y.G. and X.Y.; investigation, Y.G. and X.Y.; resources, S.L. and Y.G.; data curation, Y.G.; writing—original draft preparation, Y.G., S.L. and X.Y.; writing—review and editing, Y.G. All authors have read and agreed to the published version of the manuscript.

Funding: This work was supported by the Postgraduate Research and Practice Innovation Program of Jiangsu Province (SJCX23_1195), the Scientific Research Foundation of Nanjing Institute of Technology (ZKJ202102), and the Postgraduate Innovation Program of Nanjing Institute of Technology (TB202417075).

Institutional Review Board Statement: Not applicable.

Informed Consent Statement: Not applicable.

Data Availability Statement: The raw data supporting the conclusions of this article will be made available by the authors on request.

Conflicts of Interest: The authors declare no conflicts of interest.

References

1. Razmi, D.; Lu, T.; Papari, B.; Akbari, E.; Fathi, G.; Ghadamyari, M. An overview on power quality issues and control strategies for distribution networks with the presence of distributed generation resources. *IEEE Access* **2023**, *11*, 10308–10325.
2. Su, Q.; Li, D.; Wang, R.; Sui, Z.; Yao, J.; Shen, Q.; Yu, X. Power System with High Shares of Renewables and Power Electronics: A New Stability Criterion and Classification. *Proc. CSEE* **2024**, *44*, 3016–3036.
3. Wu, Q.; Bose, A.; Singh, C.; Chow, J.H.; Mu, G.; Sun, Y.; Liu, Y. Control and stability of large-scale power system with highly distributed renewable energy generation: Viewpoints from six aspects. *CSEE J. Power Energy Syst.* **2023**, *9*, 8–14.
4. Adetokun, B.B.; Muriithi, M.C.; Ojo, O.J. Voltage stability assessment and enhancement of power grid with increasing wind energy penetration. *Int. J. Electr. Power Energy Syst.* **2020**, *120*, 105988.
5. Meng, L.; Yang, X.; Zhu, J.; Wang, X.; Meng, X. Network partition and distributed voltage coordination control strategy of active distribution network system considering photovoltaic uncertainty. *Appl. Energy* **2024**, *362*, 122846.
6. Rahman, S.; Saha, S.; Haque, M.E.; Islam, S.N.; Arif, M.T.; Mosadeghy, M.; Oo, A.M.T. A framework to assess voltage stability of power grids with high penetration of solar PV systems. *Int. J. Electr. Power Energy Syst.* **2022**, *139*, 107815.
7. Li, S.; Lu, Y.; Ge, Y. Static voltage stability zoning analysis based on a sensitivity index reflecting the influence degree of photovoltaic power output on voltage stability. *Energies* **2023**, *16*, 2808. [CrossRef]
8. Wang, C.; Ma, J.; Shen, Y.; Peng, Y. Probabilistic load margin assessment considering forecast error of wind power generation. *Energy Rep.* **2023**, *9*, 1014–1021.

9. Li, S.; Duan, C.; Gao, Y.; Cai, Y. Classification Study of New Power System Stability Considering Stochastic Disturbance Factors. *Sustainability* **2023**, *15*, 16614. [CrossRef]
10. Li, Y.; Wan, C.; Chen, D.; Song, Y. Nonparametric Probabilistic Optimal Power Flow. *IEEE Trans. Power Syst.* **2021**, *37*, 2758–2770.
11. Hashish, M.S.; Hasanien, H.M.; Ji, H.; Alkuhayli, A.; Alharbi, M.; Akmaral, T.; Turky, R.A.; Jurado, F.; Badr, A.O. Monte Carlo simulation and a clustering technique for solving the probabilistic optimal power flow problem for hybrid renewable energy systems. *Sustainability* **2023**, *15*, 783. [CrossRef]
12. Lin, S.; Lu, Y.; Liu, M.; Yang, Y.; He, S.; Jiang, H. SVSM calculation of power system with high wind-power penetration. *IET Renew. Power Gener.* **2019**, *13*, 1391–1401. [CrossRef]
13. Ma, Y.; Luo, Z.; Zhao, S.; Wang, Z.; Xie, J.; Zeng, S. Risk assessment of a power system containing wind power and photovoltaic based on improved Monte Carlo mixed sampling. *Power Syst. Prot. Control* **2022**, *50*, 75–83.
14. Li, C.; Zhang, S.; Cheng, H.; Song, Y.; Yuan, K.; Lu, J. Correlation-based Probabilistic Multi-energy Flow Calculation of Regional Integrated Energy System with Combined Electricity and Natural Gas. *Autom. Electr. Power Syst.* **2020**, *44*, 42–49.
15. Wang, Y.; Shen, X.; Dai, Z. A probabilistic power flow calculation method considering the uncertainty of the static frequency characteristic. *Glob. Energy Interconnect.* **2019**, *2*, 45–53.
16. Zhang, Y.; Lin, S.; Yang, Y.; Liu, W.; Liu, M. Calculation of Static Voltage Stability Margin for AC/DC Hybrid Power System Considering the High-order Uncertainty of Renewable Energy. *High Volt. Eng.* **2024**, *50*, 1631–1644.
17. Zhang, R.; Jiang, T.; Li, G.; Li, X.; Chen, H. Maximum Entropy Based Probabilistic Energy Flow Calculation for Integrated Electricity and Natural Gas Systems. *Proc. CSEE* **2019**, *39*, 4430–4441.
18. Mehrdad, G.; Morteza, N.H.; Kazem, Z.; Behnam, M.I. A two-point estimate approach for energy management of multi-carrier energy systems incorporating demand response programs. *Energy* **2022**, *249*, 123671.
19. Wang, Q.; Shun, Y.; Xie, X.; Li, Y.; Xu, Q.; Zhang, Y. Probabilistic Harmonic Power Flow Algorithm Based on Improved Multi-point Estimate and Maximum Entropy. *Autom. Electr. Power Syst.* **2021**, *45*, 74–81.
20. Wang, C.; Peng, Y.; Zhou, Y.; Ma, J.; Lu, C.; Yang, X. A surrogate-assisted point estimate method for hybrid probabilistic and interval power flow in distribution networks. *Energy Rep.* **2022**, *8*, 713–721.
21. Yu, Y.; Ge, L.; Jin, C.; Wang, Y.; Ding, L. Short-term load prediction method of distribution networks considering weather features and multivariate correlations. *Power Syst. Prot. Control* **2024**, *52*, 131–141.
22. Wang, H.; Li, X.; Zou, B. Probabilistic Load Flow Calculation of Distribution System Based on Bayesian Network to Depict Wind-photovoltaic-load Correlation. *Proc. CSEE* **2019**, *39*, 4753–4763.
23. Su, C.; Liu, C.; Li, Z.; Zhou, M. Bayesian Theory Based Calculation of Probabilistic Power Flow Considering Correlation Between Multi-dimensional Wind Speed. *Autom. Electr. Power Syst.* **2021**, *45*, 157–165.
24. Lin, Z.; Wu, Q.; Chen, H.; Ji, T.; Xu, Y.; Sun, H. Scenarios-oriented distributionally robust optimization for energy and reserve scheduling. *IEEE Trans. Power Syst.* **2023**, *38*, 2943–2946.
25. Singh, V.; Moger, T.; Jena, D. Probabilistic load flow for wind integrated power system considering node power uncertainties and random branch outages. *IEEE Trans. Sustain. Energy* **2022**, *14*, 482–489.
26. Shaik, M.; Gaonkar, D.N.; Nuvvula, R.S.S.; Muyeen, S.M.; Shezan, S.A.; Shafiullah, G.M. Nataf-KernelDensity-Spline-based point estimate method for handling wind power correlation in probabilistic load flow. *Expert Syst. Appl.* **2024**, *245*, 123059.
27. Sun, Y.; Cheng, K.; Xu, Q.; Li, D.; Li, Y. Identification of Weak Link for Active Distribution Network Considering Correlation of Photovoltaic Output. *Autom. Electr. Power Syst.* **2022**, *46*, 96–103.
28. Esmaeili Shayan, M.; Najafi, G.; Ghobadian, B.; Gorjian, S.; Mamat, R.; Ghazali, M.F. Multi-microgrid optimization and energy management under boost voltage converter with Markov prediction chain and dynamic decision algorithm. *Renew. Energy* **2022**, *201*, 179–189.
29. Hasan, K.N.; Preece, R.; Milanović, J.V. Existing approaches and trends in uncertainty modelling and probabilistic stability analysis of power systems with renewable generation. *Renew. Sust. Energy Rev.* **2019**, *101*, 168–180.
30. Zhang, J.; Xiong, G.; Meng, K.; Yu, P.; Yao, G.; Dong, Z. An improved probabi listic load flow simulation method considering correlated stochastic variables. *Int. J. Electr. Power Energy Syst.* **2019**, *111*, 260–268. [CrossRef]
31. Huang, Y.; Zhang, B.; Pang, H.; Xu, J.; Liu, L.; Wang, B. Research on wind speed forecasting method based on hybrid copula optimization algorithm. *Acta Energy Sol. Sin.* **2022**, *43*, 192–201.
32. Bao, D.; Gao, F.; Wang, P.; Zhang, S.; Han, F. Research and forecasting analysis of blade load correlation based on copula function. *Acta Energy Sol. Sin.* **2023**, *44*, 323–329.
33. Philippe, W.P.; Zhang, S.; Eftekharneiad, S.; Ghosh, P.K.; Varshney, P.K. Mixed Copula-Based uncertainty modeling of hourly wind farm production for power system operational planning studies. *IEEE Access* **2020**, *8*, 138569–138583. [CrossRef]
34. Schindler, D.; Behr, H.D.; Jung, C. On the spatiotemporal variability and potential of complementarity of wind and solar resources. *Energy Conver. Manag.* **2020**, *218*, 113016.
35. Qi, J.; Yao, L.; Liao, S.; Liu, Y.; Pu, T.; Li, J.; Wang, X. Online probabilistic assessment of static voltage stability margin for power systems with a high proportion of renewable energy. *Power Syst. Prot. Control* **2023**, *51*, 47–57.
36. Zhang, X.; Pirouzi, A. Flexible energy management of storage-based renewable energy hubs in the electricity and heating networks according to point estimate method. *Energy Rep.* **2024**, *11*, 1627–1641. [CrossRef]
37. Lin, X.; Jiang, Y.; Peng, S.; Chen, H.; Tang, J.; Li, W. An efficient Nataf transformation based probabilistic power flow for high-dimensional correlated uncertainty sources in operation. *Int. J. Electr. Power Energy Syst.* **2020**, *116*, 105543. [CrossRef]

38. Ji, G.; Yuan, Y.; Fan, X.; Yuan, R.; Ling, K.; Li, X. Risk assessment of voltage limit violation on distribution network based on cornish-fisher expansion. *Acta Energy Sol. Sin.* **2020**, *41*, 358–366.
39. Xu, H.; Jiang, X.; Liu, Z.; Zou, Y.; Liao, S.; Xu, J. Probability prediction based risk assessment and proactive regulation and control strategy for static operation safety of power grid. *Autom. Electr. Power Syst.* **2022**, *46*, 182–191.
40. Wang, L.; Yuan, M.; Zhang, F.; Wang, X. Research on large scale photovoltaic planning based on risk assessment in distribution network. *J. Electr. Eng. Technol.* **2020**, *15*, 1107–1114.
41. Wang, Y.; Qiu, D.; Wang, Y.; Sun, M.; Strbac, G. Graph Learning-Based Voltage Regulation in Distribution Networks with Multi-Microgrids. *IEEE Trans. Power Syst.* **2023**, *39*, 1881–1895. [CrossRef]